


Indian saffron - Turmeric (*Curcuma longa*) embedded supermacroporous cryogel discs for heavy metal removal

Sevgi Ashyüce¹ , Nilay Bereli¹ , Aykut Topçu² , Pramod W. Ramteke³ , Adil Denizli^{1,*} 

¹Hacettepe University, Department of Chemistry, Beytepe, Ankara, Turkey

²Aksaray University, Department of Chemistry, Aksaray, Turkey

³Sam Higginbotton University of Agriculture, Technology and Science, Department of Genetics and Plant Breeding, Allahabad, India

*corresponding author e-mail address: denizli@hacettepe.edu.tr | [7101623828](https://doi.org/10.33263/BRIAC095.356361)

ABSTRACT

Cryogels are used in a variety of environmental and biotechnological processes. Cryogels are polymeric materials with large pores and open flow channels. Turmeric is a very popular spice, especially in India, which has been shown to contain curcumin alkaloids to treat a variety of many diseases. Playing a protective and therapeutic role against the diseases results from being able to bind to various targets. In this study, Indian saffron (Turmeric) embedded poly(2-hydroxyethyl methacrylate) cryogel discs (Tur-PHEMA/CDs) have been prepared to remove heavy metal ions from waste-water, which is a major environmental problem by utilizing the heavy metal binding property of turmeric. Tur-PHEMA/CDs were used to remove Cu(II), Pb(II), Cd(II) ions. Poly(2-hydroxyethyl methacrylate) cryogel discs (PHEMA/CDs) were also used as control polymer. The prepared cryogels are characterized by multiple experimental tests. The Tur-PHEMA/CDs and PHEMA/CDs with respectively swelling ratio of 83.6% and 71.2% were used in heavy metal ions adsorption studies. pH values of the solution were changed in the range of 3.0-6.0 to determine optimum pH. Maximum adsorption capacities of the Tur-PHEMA/CDs from aqueous solution were 18.36 mg/g for Cu(II), 8.99 mg/g for Pb(II) and 5.76 mg/g for Cd(II). The affinity order of heavy metal ions on mass basis was Cu(II) > Pb(II) > Cd(II) from synthetic wastewater. EDTA solution (0.5 M) was used for desorbing of heavy metal ions.

Keywords: *Indian saffron; cryogel; heavy metal ion; embedding; waste water treatment.*

1. INTRODUCTION

Turmeric is a spice obtained from the rhizomes of *Curcuma longa* (zingiberaceae). Turmeric contains an alcoholoid called curcumin, which gives the yellow color of this spice [1-3]. It is used in the treatment of many diseases in traditional Indian medicine known as Ayurveda for many years. In recent years, studies have shown that turmeric has many therapeutic properties such as cancer [4-7], inflammatory [8-10], Neurodegenerative [11-13] and cardiovascular diseases [14-16] via curcumin because of its biological targets (various enzymes, adhesion molecules, inflammatory cytokines, anti-apoptotic proteins and heavy metals).

Heavy metal pollution is one of the most important environmental problems due to toxic effects and permanent of heavy metals [17]. The amount of heavy metal ions is increasing rapidly depending on the industrial activities from natural water such as sea, lakes, rivers, etc. The heavy metals in living organisms with the ecological cycle lead to very serious health problems. For this reason, removal of heavy metals is required from environmental and waste waters [18-21].

Adsorption processes were used commonly for removing heavy metals because of high efficiency, easy to implement, low cost and

the variety rich adsorbent which are activated carbon, chitosan, cellulose and modified polymers [22-25]. In recent years, cryogels used as an adsorbent thanks to their large pores, short diffusion pathways and flexible structure [26-28]. Although there are many advantages of cryogels, low surface area and low adsorption capacity is a disadvantage. Various polymeric particles were embedded in the cryogel structure for increasing the surface area [29-32]. There are many studies for the removal of heavy metal ions and organic pollutants with the modified cryogels. These studies were included both molecular imprinting technology or various chelating groups as ligand [33-36].

In this study, we have focused our attention on combining the features of cryogels with turmeric to produce a new adsorbent system for heavy metal removal from aqueous solution. In this work, we embedded turmeric into cryogel network and used these cryogels obtained for optimizing heavy metal removal conditions. The effecting factors such as pH, ionic strength, metal ion concentration etc. were examined in the experimental studies. Finally, we performed heavy metal removal from synthetic waste water.

2. MATERIALS AND METHODS

2.1. Materials.

2-Hydroxyethyl methacrylate (HEMA), N,N'-methylenebis(acrylamide) (MBAAm) and ammonium persulfate (APS)

were purchased from Sigma (St. Louis, USA). N,N,N',N'-tetramethylene diamine (TEMED) was obtained from Fluka A.G. (Buchs, Switzerland). 1000 mg/mL stock solution of Pb(II), Cd(II)

and Cu(II) used for the adsorption experiments were prepared with their nitrate compounds. Their nitrate compounds and other chemicals were obtained from Merck AG (Darmstadt, Germany). Turmeric purchased from the local market in India. In all solutions prepared for use in the experiments was used twice distilled water from a (Dubuque, IA, USA) ROPure LP® reverse osmosis unit with a high flow cellulose acetate membrane (Barnstead D2731) followed by a Barnstead D3804 NANOpure® organic/colloid removal and ion exchange packed-bed system. 2.2. Synthesis of turmeric embedded PHEMA cryogel discs.

Firstly, monomer (1.3 mL HEMA) and crosslinker (10 mg MBAAm) were dissolved in distilled water separately, while cryogel diss containing turmeric were prepared. These two solutions were then mixed with 100 mg of turmeric and its total concentration was adjusted 6 % (w/v). Finally, to initiate the polymerization, APS (20 mg) and TEMED (25 µL) were added into this solution and the solution was mixed in ice bath for cooling. The solution was then poured into two glass panes with a 1.0 mm clearance, which was closed three sides and allowed to polymerize overnight at -12°C. The prepared cryogels were cut into discs with a diameter of 1.0 cm after they were brought to room temperature and washed.

2.2. Characterization studies.

For all characterization of the synthesized polymers, Tur-PHEMA/CDs and PHEMA/CDs were freeze-dried with a lyophilizer (Christ Alpha LD, England). The swelling rate and macroporous of the cryogels were determined by swelling tests. For this, the dry cryogels were weighed (± 0.0001 g) and their weights were recorded. The cryogels were then weighed into the vial containing 100 ml of water and weighed at regular intervals for 2 hours. Finally, the fully swollen cryogels were squeezed out and the water was removed then weighed again. Swelling ratio and macroporosity were determined using Equations 1 and 2, respectively.

$$\text{Swelling ratio (\%)} = [(W_s - W_o) / W_o] \times 100 \quad [1]$$

$$\text{Porosity (\%)} = [(W_s - W_{sq}) / W_s] \times 100 \quad [2]$$

W_o , W_s and W_{sq} are the weights (g) of cryogels before swelling, swelling and after squeezing (g), respectively.

The pore structures and the surface morphology of the pore walls (PHEMA/CDs, Tur-PHEMA/CDs) were analyzed with scanning electron microscope (SEM). Firstly, dried cryogels were grind into

fine particles and these particles were placed on a SEM sample holder separately and were covered for gold film. The samples were then placed in a SEM (FEI Quanta 200 FEG, Oregon, USA). Images of the samples were recorded at magnifications of 200-1000X to determine the cryogels and turmeric surface structure.

Fourier transform infrared spectroscopy (FTIR) was used to examine cryogels and turmeric (Perkin Elmer, Spectrum One, USA). Cryogel (2.0 mg) and turmeric (2.0 mg) were separately mixed with 98 mg of KBr and pelleted to prepare samples for FTIR analysis and than spectrums were recorded between 4000-450 cm^{-1} .

2.3. Removal of heavy metal ions from aqueous solutions

The Tur-PHEMA/CDs retention performance of metal ions was studied using aqueous solutions of Cd(II), Cu(II) and Pb(II). Adsorption experiments were performed in a batch system at 11 different concentrations ranging from 10-2000 mg/mL. Cryogels with a dry weight of 14.5 mg were treated for 120 min at 20 rpm on a rotator with 5 ml of different concentrations of these metals. In order to observe the effect of pH change on the removal of heavy metal ions from the aqueous solution, in order to observe the effect of pH change on the removal of heavy metals from the aqueous solution, cryogels were treated with aqueous solutions containing heavy metals at a pH range of 3-6. The Tur-PHEMA/CDs were used as a control polymer which was used all adsorption studies in batch system as well. 50 mM EDTA was used as desorption solution for 1 hour. The concentrations of the metal ions in the aqueous solutions at the beginning, the end of the experiment, the end of desorption and the desired time intervals were measured by flame atomic absorption spectrophotometer (AAS, Analyst 800/Perkin Elmer).

2.4. Removal of heavy metal ions from synthetic wastewater.

Synthetic wastewater contains 50 mg/L from each metal ions [Cd(II), Pb(II), Cu(II)] and 0.1 mmol/L Ni(II), Zn(II), Fe(II), Co(II), Sn(II), Ag(I) were used to the heavy metal ion removal of Tur-PHEMA/CDs from complex mixture under competitive manner. NaCl (700 mg/L) was added into the synthetic wastewater to adjust salinity. As a result of adsorption studies from synthetic wastewater carried out in the same way as aqueous solution studies and ion concentrations were measured by AAS.

3. RESULTS

3.1. Characterization studies

Swelling test showed that the swelling ratio and porosity of PHEMA/CDs and Tur-PHEMA/CDs are 785% and 841% swelling ratio, 86.3% and 71.2% porosity respectively.

Figure 1 shows the optical photographs of the turmeric, PHEMA/CDs and Tur-PHEMA/CDs. As the photograph, color of PHEMA cryogel was turned yellow because of the embedding of turmeric on the PHEMA cryogel. SEM images of PHEMA/CDs and Tur-PHEMA/CDs were given in Figure 2. As it is clear from the images, turmeric was embedded successfully into the PHEMA cryogel. In addition to the cryogels pore sizes were the range of about 40-100 µm.

FTIR spectrum of turmeric, PHEMA/CDs and Tur-PHEMA/CDs were shown in Figure 3. For turmeric, the band at 1630 cm^{-1} has largely mixed C=C and C=O vibration modes. The bant at 1513

cm^{-1} was most important, which was based on highly mixed vibration (C=O, CC=O). The band at 1283 cm^{-1} was occurred due to the C-H vibrations of aromatic rings. In addition, the band at 856 cm^{-1} was associated with C-H and CCH aromatic rings vibrations. Obtained results of FTIR spectra of Turmeric are consistent with literature for enol form of curcumin. FTIR spectra of PHEMA, there are three special peak to explain the spectrum, which are 3416 cm^{-1} , 2951 cm^{-1} and 1725 cm^{-1} due to O-H, C-H, C=O starching vibration respectively.

3.2. Adsorption Studies.

3.2.1. Effect of pH. pH is an important factor, that it affects the binding of metal ions on the adsorbent. Because of this, experiments were performed various pH value (pH 3.0-6.0). In this experiment, initial concentration of each metal ion was 10 mg/L and due to the metal ions are collapsed over pH 6.0, that the

value of pH was used maximum 6.0. As seen in Figure 3A, maximum adsorption amount of Cu(II), Pb(II) and Cd(II) were about 0.350 mg/g, 0.274 mg/g and 0.190 mg/g respectively, they were observed pH 5.0. Thus, subsequent experiments were performed value of pH 5.0.

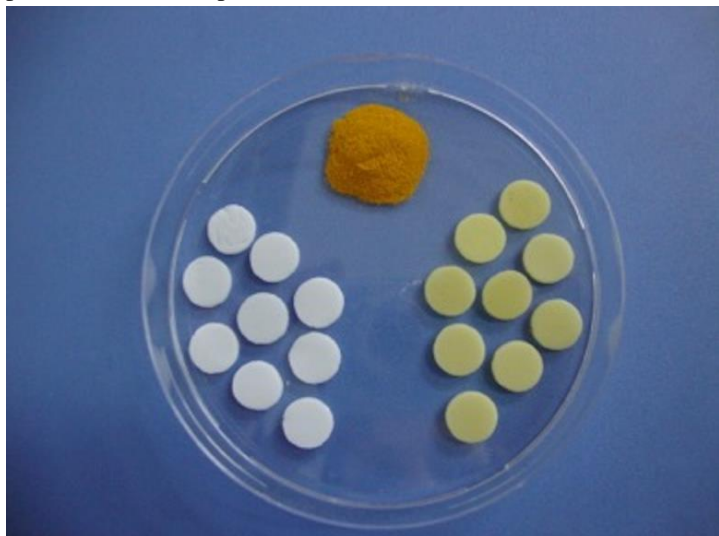


Figure 1. Optical photographs of the Turmeric (A), PHEMA/CDs (B) and Tur-PHEMA/CDs.

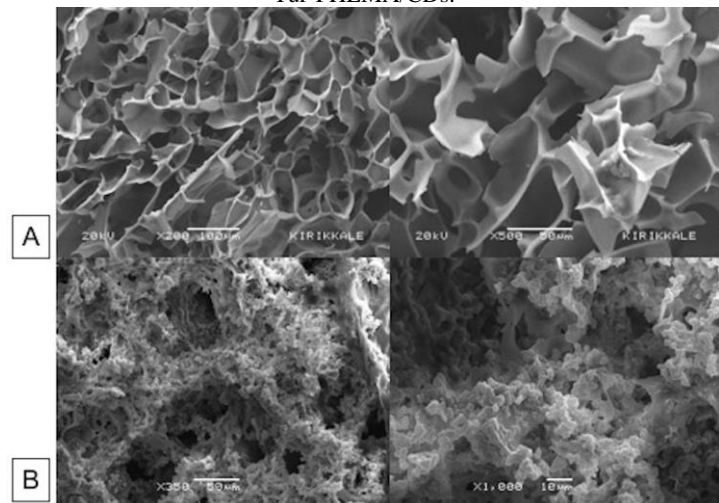


Figure 2. SEM images of PHEMA/CDs (A) and Tur-PHEMA/CDs (B).

3.2.2. Adsorption rate. Adsorption rate is an important parameter, which explains the interaction between heavy metal ions and adsorbent. Initial heavy metal ion concentration was selected 50 mg/L and the value of medium pH 5.0 was selected for performed experiment to determine the adsorption rate. As seen in Figure 3B, adsorption rate of each heavy metal ions on Tur-PHEMA/CDs was increased rapidly at the first 60 minute. After 60 min adsorption rate was fixed at 0.720 mg/g for Cu(II), 0.670 mg/g for Pb(II) and 0.435 mg/g for Cd(II) because of the filling all metal binding side of the adsorbent. It can be said that the rapid adsorption is most likely due to high affinity between heavy metal ions and Tur-PHEMA/CDs.

3.2.3. Adsorption Capacity. In this experiment to determine the adsorption capacity of Tur-PHEMA/CDs were used 11 different concentrations for each heavy metal ion, that they were in the range of 10-2000 mg/L. As seen in Figure 3C, adsorption amounts of heavy metal ions were increased rapidly up to 1000 mg/L concentration but after the 1000 mg/L due to the filling all the metal binding area on the surface of adsorbent, when the quantities of adsorption were fixed. According to the results, maximum

adsorption capacity of Tur-PHEMA/CDs was about 18.3 mg/g, 8.9 mg/g, 5.7 mg/g for Cu(II), Pb(II), Cd(II) respectively. On the other hand, adsorption amount of heavy metal ions can be ordered Cu(II) (279 µmol/g) > Cd(II) (50.7 µmol/g) > Pb(II) (43.4 µmol/g) when analyzed as molar basis.

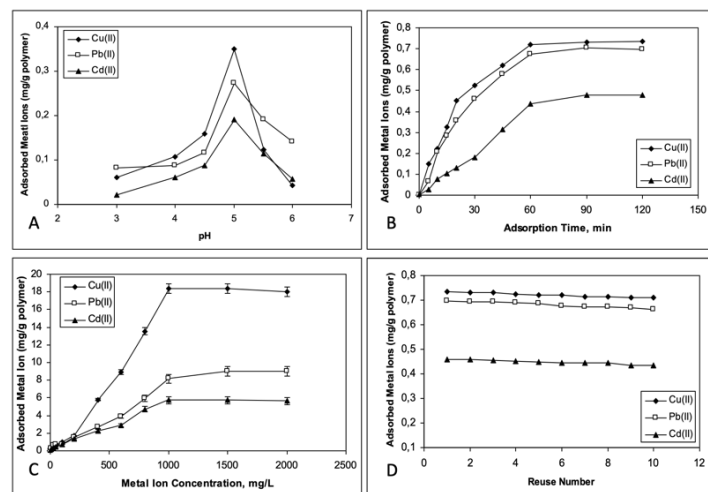


Figure 3. Effect of pH on adsorption of metal ions on Tur-PHEMA/CDs: concentration of metal ions: 10 mg/L; T: 25°C (A), adsorption rates of heavy metal ions by Tur-PHEMA/CDs: concentration of metal ions: 50 mg/L; pH: 5.0; T: 25°C (B), adsorption capacity of the Tur-PHEMA/CDs for metal ions: pH: 5.0; T: 25°C (C) and adsorption-desorption cycle of the Tur-PHEMA/CDs: metal ions concentration: 50 mg/L; pH: 5.0; T: 25°C (D).

Adsorption isotherms are used to explain the correlation between the adsorption capacity on adsorbent and solute concentration, when the two phases are equilibrium. In this study, Langmuir and Freundlich were used as binding isotherms to explain the relationship between each metal ion and Tur-PHEMA/CDs. The Langmuir model considers monolayer adsorption over homogeneous adsorbent area. Freundlich isotherm theory is an exponential equation, thereupon with increasing adsorbate concentration also increases adsorption on the adsorption surface. The equations of Langmuir and Freundlich isotherms have been shown in previous studies. As seen in Table 1, the isotherm data was appropriate Langmuir model [$R^2=0.976$ for Cu(II), $R^2=0.992$ for Pb(II), $R^2=0.984$ for Cd(II)] rather than Freundlich model [$R^2=0.936$ for Cu(II), $R^2=0.971$ for Pb(II), $R^2=0.969$ for Cd(II)]. According to the Langmuir isotherms, theoretical values of maximum adsorption (Q_{max}) were close to the experimental values for each metal ion.

3.2.4. Desorption and Repeated Use. It can be used again without losing the effectiveness of adsorbent is of great importance in economic terms. In this experiment, 10 recurrent adsorption-desorption were done for each heavy metal ion on the same cryogels, which was tested the reusability of Tur-PHEMA/CDs. 0.5 M EDTA was used for 1 has an elution solution. Adsorption amounts of heavy metals for consecutively 10 cycles were given in Figure 3D. As the calculations, the adsorption capacities of Tur-PHEMA/CDs were decreased after 10 cycles just about 3-5% for each heavy metal ions. According to these results it can be said, 0.5 M EDTA was appropriate adsorption agent and Tur-PHEMA/CDs can be used repeatedly.

Heavy metal chelation on the adsorbent was made a comparison with control polymer. In Figure 4A was given a comparison of adsorption capacities of PHEMA/CDs and Tur-PHEMA/CDs. As shown, adsorption capacity of Tur-PHEMA/CDs for Cu(II) 7.58

times, for Pb(II) 12.45 times and for Cd(II) 4.42 times more than PHEMA/CDs.

3.2.5. Adsorption from Synthetic Wastewater. Multi-component heavy metal adsorption studies were performed from synthetic waste water. In a competitive system there are three types of responses in heavy metal mixture that they are synergism, antagonism and non-interaction. Comparison of non-competitive and competitive adsorptions amounts of Cu(II), Pb(II) and Cd(II)

ions was shown in Figure 4. They were determined respectively as about 1.075 mg/g, 0.400 mg/g and 0.300 mg/g. As seen, the adsorption amount of Cu(II) from synthetic waste water was higher than the single solutions, which is means synergism. As distinct from Cu(II), in heavy metal mixture occurred antagonism for Pb(II) and Cd(II), that their adsorption amounts from heavy metal mixture were lower than the single solution.

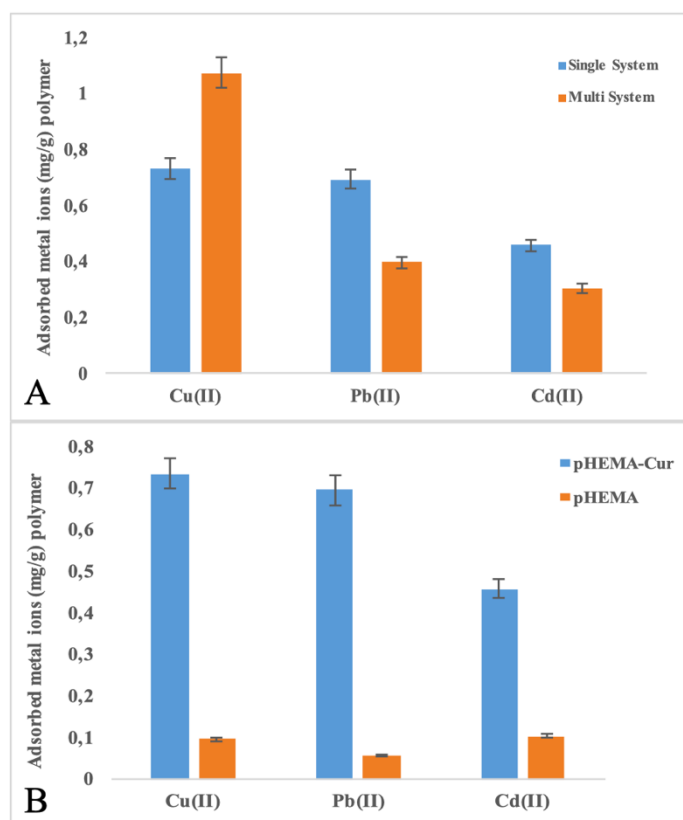


Figure 4. Adsorption capacity of the Tur-PHEMA/CDs for metal ions: pH: 5.0; T: 25°C (A) and comparison of adsorption capacities of the PHEMA/CDs and Tur-PHEMA/CDs: pH: 5.0; initial concentrations of metal ions: 50 mg/L; T: 25°C (B).

Table 1. Langmuir and Freundlich adsorption isotherm constants.

Metal ions	Experimental Q (mg/g)	Langmuir			Freundlich		
		Q _{max} (mg/g)	b (mL/mg)	R ²	K _F	1/n	R ²
Cu ²⁺	18.02	22.47	9.47	0.976	44.7	0.851	0.936
Pb ²⁺	8.99	8.03	1.93	0.992	181.4	0.646	0.971
Cd ²⁺	5.65	3.25	38	0.984	2.08	0.595	0.969

4. CONCLUSIONS

In this study, the cryogel, which has a large pore size, high physical and chemical structure were combined Turmeric, which contains curcumin alcohol and used as a natural ligand for heavy metal removing. Turmeric embedding cryogel used successfully capture heavy metal ions from aqueous solution and even synthetic waste water. On the other hand, synthesized cryogels can

be used in many times, therefore these polymers have a low cost. It is concluded that synthesis of economically and structurally advantageous materials by this study, which can be used in waste water for heavy metal ions removing, which are hazardous materials for environment.

5. REFERENCES

1. Gilda, S.; Kanitkar, M.; Bhone, R.; Paradkar, A. Activity of water-soluble turmeric extract using hydrophilic excipients. *LWT-Food Sci. Technol.* **2010**, *43*, 59-66, <https://doi.org/10.1016/j.lwt.2009.07.004>.
 2. Ratanajajaroen, P.; Watthanaphanit, A.; Tamura, H.; Tokura, S.; Rujiravanit, R. Release characteristic and stability of curcumin incorporated in β-chitin non-woven fibrous sheet using

Tween 20 as an emulsifier. *Eur. Polym. J.* **2012**, *48*, 512-523, <https://doi.org/10.1016/j.eurpolymj.2011.11.020>.
 3. Li, H.; Sureda, A.; Devkota, H.P.; Pittalà, V.; Barreca, D.; Silva, A.S.; Tevari, D.; Xu, S.; Nabavi, S.M. Curcumin, the golden spice in treating cardiovascular diseases. *Biotechnol. Adv.* **2019**, <https://doi.org/10.1016/j.biotechadv.2019.01.010>.

4. Mirzaei, H.; Masoudifar, A.; Sahebkar, A.; Zare, N.; Sadri Nahand, J.; Rashidi, B.; Jaafari, M.R. MicroRNA: A novel target of curcumin in cancer therapy. *J. Cell. Physiol.* **2018**, *233*, 3004-3015, <https://doi.org/10.1002/jcp.26055>.
5. Panda, A. K.; Chakraborty, D.; Sarkar, I.; Khan, T.; Sa, G. New insights into therapeutic activity and anticancer properties of curcumin. *J. Exp. Pharm.* **2017**, *9*, 31, <https://doi.org/10.2147/JEP.S70568>.
6. Gawde, K.A.; Sau, S.; Tatiparti, K.; Kashaw, S.K.; Mehrmohammadi, M.; Azmi, A.S.; Iyer, A.K. Paclitaxel and di-fluorinated curcumin loaded in albumin nanoparticles for targeted synergistic combination therapy of ovarian and cervical cancers. *Colloid. Surface. B.* **2018**, *167*, 8-19, <https://doi.org/10.1016/j.colsurfb.2018.03.046>.
7. Karimian, S.M.; Pirro, M.; Johnston, P.T.; Majeed, M.; Sahebkar, A. Curcumin and endothelial function: evidence and mechanisms of protective effects. *Curr. Pharm. Design.* **2017**, *23*, 2462-2473, <https://doi.org/10.2174/1381612823666170222122822>.
8. Deguchi, Y.; Andoh, A.; Inatomi, O.; Yagi, Y.; Bamba, S.; Araki, Y.; Fujiyama, Y. Curcumin prevents the development of dextran sulfate Sodium (DSS)-induced experimental colitis. *Digest. Dis. Sci.* **2007**, *52*, 2993-2998, <https://doi.org/10.1007/s10620-006-9138-9>.
9. Ghosh, S.; Banerjee, S.; Sil, P.C. The beneficial role of curcumin on inflammation, diabetes and neurodegenerative disease: A recent update. *Food Chem. Toxicol.* **2015**, *83*, 111-124, <https://doi.org/10.1016/j.fct.2015.05.022>.
10. Larmonier, C.B.; Uno, J.K.; Larmonier, N.; Midura, A.J.; Timmermann, B.; Ghishan, F.K.; Kiela, P.R. Protective effects of dietary curcumin in mouse model of chemically induced colitis are strain dependent. *Inflamm. Bowel. Dis.* **2008**, *14*, 780-793, <https://doi.org/10.1002/ibd.20348>.
11. Reddy, P.H.; Manczak, M.; Yin, X.; Grady, M.C.; Mitchell, A.; Tonk, S.; Kumar, S. Protective effects of Indian spice curcumin against amyloid- β in Alzheimer's disease. *J. of Alzheimers Dis.* **2018**, *61*, 843-866, <https://doi.org/10.3233/JAD-170512>.
12. Serafini, M.M.; Catanzaro, M.; Rosini, M.; Racchi, M.; Lanni, C. Curcumin in Alzheimer's disease: Can we think to new strategies and perspectives for this molecule? *Pharmacological research* **2017**, *124*, 146-155, <https://doi.org/10.1016/j.phrs.2017.08.004>.
13. Ono, K.; Hasegawa, K.; Naiki, H.; Yamada, M. Curcumin has potent anti-amyloidogenic effects for Alzheimer's β -amyloid fibrils in vitro. *J. Neurosci. Res.* **2004**, *75*, 742-750, <https://doi.org/10.1002/jnr.20025>.
14. Quiles, J.L.; Mesa, M.D.; Ramírez-Tortosa, C.L.; Aguilera, C.M.; Battino, M.; Gil Á.; Ramírez-Tortosa, M.C. Curcuma longa extract supplementation reduces oxidative stress and attenuates aortic fatty streak development in rabbits. *Arterioscl. Throm. Vas. Biol.* **2002**, *22*, 1225-1231, <https://doi.org/10.1161/01.ATV.0000020676.11586.F2>.
15. Venkatesan, N. Curcumin attenuation of acute adriamycin myocardial toxicity in rats. *Brit. J. Pharmacol.* **1998**, *124*, 425-427, <https://doi.org/10.1038/sj.bjp.0701877>.
16. Yang, X.; Thomas, D.P.; Zhang, X.; Culver, B.W.; Alexander, B.M.; Murdoch, W.J.; Sreejayan, N. Curcumin inhibits Platelet-derived growth factor-stimulated vascular smooth muscle cell function and Injury-induced neointima Formatio. *Arterioscl. Throm. Vas. Bio.* **2006**, *26*, 85-90, <https://doi.org/10.1161/01.ATV.0000191635.00744.b6>.
17. Erdem, Ö.; Saylan, Y.; Andaç, M.; Denizli, A. Molecularly imprinted polymers for removal of metal ions: an alternative treatment method, *Biomimetics* **2018**, *3*, 3040038, <https://doi.org/10.3390/biomimetics3040038>.
18. Kar, D.; Sur, P.; Mandai, S.K.; Saha, T.; Kole, R.K.; Assessment of heavy metal pollution in surface water. *Int. J. Environ. Sci. Technol.* **2008**, *5*, 119-124, <https://doi.org/10.1007/BF03326004>.
19. Gurgel, L.V.A.; Júnior, O.K.; Freitas, Gil R.P.; Gil, L.F. Adsorption of Cu (II), Cd (II), and Pb (II) from aqueous single metal solutions by cellulose and mercerized cellulose chemically modified with succinic anhydride. *Bioresource. Technol.* **2008**, *99*, 3077-3083, <https://doi.org/10.1016/j.biortech.2007.05.072>.
20. Karakoç, V.; Andaç, M.; Denizli, A.A. Molecularly imprinted nanoparticles for the removal of srsenic from environmental water sources, In: *Nanomaterials for Water Remediation: Carbon-Based Materials*, A.K. Misra, ed., Volume 1, **2016**; pp. 161-184, Smithers Rapra Publ., Shawbury, UK.
21. Sağlam, A.; Demir, A.; Bektaş, S.; Denizli, A. *Ion-imprinted thermosensitive cryogels for heavy metal removal*, in: *Nanomaterials for Water Remediation: Inorganic Oxide Materials*, A.K. Misra, ed., Volume 2, **2016**, pp. 145-170, Smithers Rapra Publ., Shawbury, England.
22. Kadirvelu, K.; Thamaraiselvi, K.; Namasivayam, C. Removal of heavy metals from industrial wastewaters by adsorption onto activated carbon prepared from an agricultural solid waste. *Bioresource. Technol.* **2001**, *76*, 63-65, [https://doi.org/10.1016/S0960-8524\(00\)00072-9](https://doi.org/10.1016/S0960-8524(00)00072-9).
23. Liu, X.; Hu, Q.; Fang, Z.; Zhang, X.; Zhang, B. Magnetic chitosan nanocomposites: a useful recyclable tool for heavy metal ion removal. *Langmuir* **2008**, *25*, 3-8, <https://doi.org/10.1021/la802754t>.
24. Safarik, I.; Safarikova, M. Magnetic fluid modified peanut husks as an adsorbent for organic dyes removal. *Phys. Procedia.* **2010**, *9*, 274-278, <https://doi.org/10.1016/j.phpro.2010.11.061>.
25. Tamahkar, E.; Türkmen, D.; Akgönüllü, S.; Qureshi, T.; Denizli, A. *Modified bacterial cellulose nanofibers applied for mercury contamination removal from water sources*, in: *Nanotechnology for Sustainable Water Resources*, A.K. Misra and C.M. Hussain, eds., Chapter 16, **2018**; pp. 501-523, Scrivener Publ., Wiley.
26. Noir, M.L.; Plieva, F.; Hey, T.; Guieysse, B.; Mattiasson, B. Macroporous molecularly imprinted polymer/cryogel composite systems for the removal of endocrine disrupting trace contaminants. *J. Chromatogr. A* **2007**, *1154*, 158-164, <https://doi.org/10.1016/j.chroma.2007.03.064>.
27. Zhao, S.; Zou, Y.; Wang, Y.; Zhang, H.; Liu, X. Organized cryogel composites with 3D hierarchical porosity as an extraction adsorbent for nucleosides. *J. Sep. Sci.* **2019**, *42* 2140-2147, <https://doi.org/10.1002/jssc.201900174>.
28. Alkan, H.; Bereli, N.; Baysal, Z.; Denizli, A. Antibody purification with protein A attached supermacroporous poly (hydroxyethyl methacrylate) cryogel. *Biochem. Eng. J.* **2009**, *45*, 201-208, <https://doi.org/10.1016/j.bej.2009.03.013>.
29. Aslyüce, S.; Uzun, L.; Rad, A.Y.; Unal, S.; Say, R.; Denizli, A. Molecular imprinting based composite cryogel membranes for purification of anti-hepatitis B surface antibody by fast protein liquid chromatography. *J. Chromatogr. B* **2012**, *889*, 95-102, <https://doi.org/10.1016/j.jchromb.2012.02.001>.
30. Baydemir, G.; Bereli, N.; Andaç, M.; Say, R.; Galaev, I.Y.; Denizli, A. Supermacroporous poly (hydroxyethyl methacrylate) based cryogel with embedded bilirubin imprinted particles. *React. Funct. Polym.* **2009**, *69*, 36-42, <https://doi.org/10.1016/j.reactfunctpolym.2008.10.007>.
31. Koç, İ.; Baydemir, G.; Bayram, E.; Yavuz, H.; Denizli, A. Selective removal of 17 β -estradiol with molecularly imprinted particle-embedded cryogel systems, *J. Hazard. Mater.* **2011**, *192*, 1819-1826, <https://doi.org/10.1016/j.jhazmat.2011.07.017>.
32. Shaikh, H.; Andaç, M.; Memon, N.; Bhangar, M.I.; Nizamani, S.M.; Denizli, A. Synthesis and characterization of molecularly imprinted polymer embedded composite cryogel

discs: application for the selective extraction of cypermethrins from aqueous samples prior to GC-MS analysis. *RSC Adv.* **2015**, *5*, 26604-26615, <https://doi.org/10.1039/C4RA13318H>.

33. Bereli, N.; Andaç, M.; Baydemir, G.; Say, R.; Galaev, I.Y.; Denizli, A., Protein recognition via ion-coordinated molecularly imprinted supermacroporous cryogels. *J. Chromatogr. A.* **2008**, *1190*, 18-26, <https://doi.org/10.1016/j.chroma.2008.02.110>.

34. Ashyüce, S.; Bereli, N.; Uzun, L.; Onur, M.A.; Say, R.; Denizli, A. Ion-imprinted supermacroporous cryogel, for in vitro removal of iron out of human plasma with beta thalassemia. *Sep. Purif. Technol.* **2010**, *73*, 243-249, <https://doi.org/10.1016/j.seppur.2010.04.007>.

35. Tekin, K.; Uzun, L.; Şahin, Ç.A.; Bektaş, S.; Denizli, A. Preparation and characterization of composite cryogels containing imidazole group and use in heavy metal removal. *React. Funct. Polym.* **2011**, *71*, 985-993, <https://doi.org/10.1016/j.reactfunctpolym.2011.06.005>.

36. Önnby, L.; Giorgi, C.; Plieva, F.M.; Mattiasson, B. Removal of heavy metals from water effluents using supermacroporous metal chelating cryogels. *Biotechnol. Progr.* **2010**, *26*, 1295-1302, <https://doi.org/10.1002/btpr.422>.

37. Uzun, L.; Kara, A.; Osman, B.; Yılmaz, E.; Beşirli, N.; Denizli, A. Removal of heavy-metal ions by magnetic beads containing triazole chelating groups. *J. Appl. Polym. Sci.* **2009**, *114*, 2246-2253, <https://doi.org/10.1002/app.30511>.



© 2019 by the authors. This article is an open access article distributed under the terms and conditions of the Creative Commons Attribution (CC BY) license (<http://creativecommons.org/licenses/by/4.0/>).